BMC Genomics

RESEARCH Open Access

Identification of key genes and metabolites involved in intramuscular fat deposition in Laiwu pigs through combined transcriptomic and lipidomic analyses

Wen Chuan Peng[1†], Guo He Cai[2†], Rui Rui Pan[1], Yong Zhen Niu[1], Jun Ying Xiao[1], Chu Xiong Zhang[1], Xiao Zhang[1] and Jiang Wei Wu[1*]

Abstract

Pork quality is a key goal in commercial pig farming. Intramuscular fat (IMF) content in pigs serves as a critical determinant of meat quality, yet its regulatory mechanism remains unclear. In this study, two different pig breeds Chinese native breed Laiwu (fatty-type) and Yorkshire (lean-type), were selected as research subjects. The molecular regulatory mechanisms affecting IMF content were investigated through integrated transcriptomic and lipidomic analysis. We identified critical genes, including ACC1, FASN, ELOVL6, SCD, and DGAT2, and elucidated their synergistic interactions in promoting IMF deposition in Laiwu pigs. The findings reveal that the coordinated action of genes such as ACC1 and FASN promotes the increased production of palmitic acid, which was subsequently elongated and desaturated by ELOVL6 and SCD to form long-chain fatty acids necessary for TG synthesis. Additionally, DGAT2 facilitates the extensive synthesis of TG, which is stored in lipid droplets under the regulation of PLIN1. This increased triglyceride synthesis and storage capacities in Laiwu pigs, functioning as one of the key factors contributing to its high IMF content. The study highlights the importance of gene-lipid interactions in IMF deposition and offers novel insights into the genetic and molecular basis of IMF accumulation, particularly in fatty pig breeds like the Laiwu. Our research findings provide new directions for developing targeted genetic or nutritional interventions to enhance IMF content and improve meat quality.

Keywords Pigs, Intramuscular fat, Longissimus thoracis, Gene-lipid interaction network

[†]Wen Chuan Peng and Guo He Cai contributed equally to this work.

*Correspondence:
Jiang Wei Wu
wujiangwei@nwafu.edu.cn
[1]Key Laboratory of Animal Genetics Breeding and Reproduction of Shaanxi Province College of Animal Science and Technology Northwest A&F University Yangling, Shaanxi 712100, China
[2]The Key Laboratory of Healthy Mariculture for the East China Sea, Ministry of Agriculture, Fisheries College, Ji Mei University, Xiamen 361021, China

Introduction

Pork stands as a significant source of meat in human diets, with increasing consumer awareness regarding meat quality. Among the various determinants of meat quality, intramuscular fat (IMF) plays a decisive role, as it is closely associated with key attributes such as tenderness, flavor, juiciness, and marbling. IMF is the fat deposited between muscle fibers, and its level significantly influences the sensory characteristics and overall palatability of pork, making it a crucial factor in the breeding and management of pigs for high-quality meat production [1–5]. The IMF content positively influences meat quality traits. A high IMF content results in better meat flavor, whereas a low IMF content results in a decrease in flavor precursors [6]. Low IMF is the outcome of high-intensity and long-term selection for fat deposition and growth rate traits in conventional Western pig breeds like Yorkshire and Landrace pigs [7]. IMF content in Laiwu pigs (13.83%) is significantly higher than that in Yorkshire pigs (1.54%) [8]. Similarly, when compared to other Chinese indigenous breeds, such as Erhualian and Bama, Laiwu pigs also demonstrated significantly higher IMF levels, with an average of 10.3% and a maximum value of up to 17.8% [9]. This unique characteristic makes Laiwu pigs an ideal model for studying IMF deposition and its impact on meat quality. In recent years, multi-omics approaches have become increasingly prominent for investigating the molecular mechanisms underlying complex traits, including meat quality [10]. These powerful technologies have proven highly effective in examining the genetic and biochemical foundations of meat quality traits. Several candidate genes implicated in IMF content have been identified in Duroc pigs, such as *ADIPOQ*, *PPARγ*, *LIPE*, *CIDEC*, *PLIN1*, *CIDEA*, and *FABP4* [11]. The identification of key genes involved in regulating IMF deposition in the longissimus dorsi muscle of Dingyuan pigs has been facilitated by transcriptomics and proteomics [12]. Furthermore, research has pinpointed candidate long non-coding RNAs and mRNAs associated with IMF in Laiwu pigs [13]. In addition, the combination of metabolomics and lipidomics has enabled the identification of flavor precursors and biomarkers in Laiwu pigs [14]. Despite these advancements, uncovering the full spectrum of molecular mechanisms governing variations in meat quality, particularly those related to fat deposition, remains a formidable challenge. This complexity arises from the multifaceted nature of fat metabolism and its intricate interactions with genetic, epigenetic, and environmental factors. Further research employing integrated multi-omics strategies is crucial for achieving a more comprehensive understanding of these processes. Transcriptomics offers in-depth insights into the genetic regulatory processes at the transcriptional level [15], while lipidomics provides complementary insights at the metabolic level [16, 17]. Therefore, the combined application of transcriptomics and lipidomics will aid in developing more precise and effective strategies to improve meat quality.

While the relationship between meat quality and IMF has been extensively studied, the molecular mechanisms responsible for differences in fat deposition between native Chinese breeds and commercially lean pig breeds remain poorly understood. In this study, we employed integrated transcriptomic and lipidomic analyses to explore the factors contributing to the variations in IMF content between Laiwu and Yorkshire pigs. Our findings provide valuable insights into the genetic and biochemical bases of IMF regulation, which could pave the way for strategies to enhance IMF deposition in pork production.

Materials and methods

Ethics statement

This study received approval from the Animal Ethics Committee of College of Animal Science & Technology, Northwest A&F University (XN2023-1005).

Animals and sample collection

The animals used in our study were purchased by the researchers from Shandong Province Laiwu Pig Original Seed Co., Ltd. (Shandong, China). The temperature in the facility was maintained at 22–24 °C with a relative humidity of 55–60%. Throughout the experiment, pigs have free access to food and water. The feed was made of commercial soybean meal and corn (Beijing Great North Agricultural Technology Group Co., Ltd., Beijing, China). The feed formulations were presented in Table S1. All experiments were carried out by the researchers and the experimental groups were blinded in order to maintain objectivity. A total of 24 pigs comprising 12 Yorkshire pigs and 12 Laiwu pigs were used in this study. They were divided into two cohorts. The first cohort, consisting of 6 Laiwu and 6 Yorkshire pigs with similar age (about 7 months old), was housed together throughout the entire experiment. This cohort was used for comparisons between two pig breeds based on similar age. The second cohort, also consisting of 6 Laiwu and 6 Yorkshire pigs with similar body weight, was used for comparisons between two pig breeds based on similar body weight (110 ± 1.12 kg). The animals were maintained following standard husbandry practices to ensure the scientific rigor and reproducibility of the results. Backfat thickness was assessed using A-mode ultrasound (Renco Co., MN, USA). A-mode is currently used for creating images from which fat thickness and other carcass characteristics are calculated. Once the performance tests were completed, samples were taken from different sites including the front (fifth rib), middle (last rib) as well as back (last lumbar bone). Pigs underwent fasting for 12 h

before slaughter. Plasma samples were obtained from the anterior vena cava, and the pigs were euthanized by electroshock, followed by exsanguination. Subcutaneous fat, longissimus thoracis, and mesenteric fat tissues intended for RNA and western blot analysis were promptly isolated and preserved in liquid nitrogen. For histological analyses (H&E staining), longissimus thoracis was fixed in 4% paraformaldehyde.

Transcriptomics data analysis and real-time qPCR

Transcriptomics was completed by LC Biotechnology Co., Ltd. (Hangzhou, China). The porcine reference genome version was *Sus scrofa 11.1*. Screening criteria were Fold Change (FC) ≥ 2 or FC ≤ 0.5 and p-value < 0.05. The raw sequence data for transcriptomics have been submitted to the NCBI Gene Expression Omnibus (GEO) datasets with accession number GSE268121. Around 50 mg of frozen tissues were grinded in liquid nitrogen and then transferred into 1 mL of Trizol regent (Takara, Kyoto, Japan) for RNA extraction according to the manufacturer's instructions. Complementary DNA (cDNA) was synthesized from total RNA using cDNA synthesis kit (R333-01, Vazyme Biotech, Nanjing, China) following the manufacturer's instructions. RT-qPCR was performed using a CFX 96 Real-Time PCR Detection System (Bio-Rad, Hercules, California, USA). Each 20 mL amplifications contained 10 μL of ChamQ SYBR qPCR Master Mix (Q222-01, Vazyme Biotech), 7.8 mL of sterilized double-distilled water, 1 mL of 1:10 diluted cDNA, and 0.6 mL of each forward and reverse primer. The RT-qPCR program comprised an initial activation step at 95 °C for 3 min, followed by 38 cycles of 95 °C for 15 s and 60 °C for 30 s, and 5 s at 65 °C. After the PCR, a single product generated in these reactions was confirmed via melting curve analyses. RT-qPCR was conducted according to the described method [18]. Primer sequences were shown in Table S2.

Lipid mass spectrometric analyses

Lipidomics was conducted by LC Biotechnology Co., Ltd. (Hangzhou, China). According to previous research methods, the data were normalized and analyzed by metaX [19–22], and lipids were evaluated using a variable importance in projection (VIP) scores [23]. FC ≥ 1.5 or FC ≤ 1/1.5, VIP ≥ 1 and p-values < 0.05 were utilized in the analysis. The lipidomics data from this study are stored in the EMBL-EBl MetaboLights database (MTBLS10230).

Integrative transcriptomics and lipidomics analyses

The detailed procedure for the combined analysis is as follows. First, differentially expressed genes (DEGs) from the transcriptome were identified using the thresholds of p-value < 0.05 and FC ≥ 2 or FC ≤ 0.5. Subsequently, KEGG pathway enrichment analysis was performed on these DEGs to identify the enriched pathways. Similarly, differentially abundant lipids were selected using the thresholds of p-value < 0.05, FC ≥ 1.5 or FC ≤ 1/1.5, and VIP ≥ 1. KEGG pathway enrichment analysis was then conducted on the differentially abundant lipids to identify the enriched pathways. Finally, a Venn diagram was used to compare the pathways enriched in both transcriptomic and lipidomic datasets, allowing identification of the common pathways.

Measurment of plasma lipids

Plasma triglycerides (TGs) were detected using commercial kits (#1488872; Roche Diagnostics; 80-INSMSU-E01, Alpco Diagnostics). Low-density lipoprotein (LDL), high-density lipoprotein (HDL), as well as free fatty acid (FFA) were identified through a clinical autoanalyzer (Beckman Coulter DX) at hospital.

Crude fat content of longissimus thoracis

The crude fat content of the longissimus thoracis was measured using Soxhlet extraction [24]. First, the sample is dried, ground into a fine powder, and weighed before being placed into the extraction flask. Second, ether is added to the weighed extraction flask, and the mixture is heated under reflux for 6–8 h. Finally, the solvent is recovered, and the extraction flask is dried, cooled, and weighed again. The fat content is then calculated based on the mass difference before and after extraction. All steps must be performed in a fume hood to ensure safety.

Western blot

Longissimus thoracis muscle and subcutaneous fat were washed with PBS and lysed in RIPA lysis buffer (P0013C, Beyotime Biotechnology, Shanghai, PRC). Next, 200 μg of total protein was resolved by 10% or 12% sodium dodecyl sulfate-polyacrylamide gel electrophoresis (SDS-PAGE) electrophoresis and transferred onto a polyvinylidene fluoride (PVDF) (IPVH00010, Millipore, Massachusetts, USA) membrane via electroblotting. The PVDF membrane was blocked in black buffer (5% skim milk powder dissolved in TBST) for 2 h at room temperature. The primary antibodies shown in Table S3 were inoculated at 4˚C overnight. Subsequently, the PVDF membrane was washed 4 times with TBST (5 min per time) and stained with the secondary antibodies (goat anti-rabbit or mouse) for 2 h at room temperature. After washing with TBST, the ECL Reagent (WBKlS0100, Millipore) was used, and the strips were on film. Western blot was carried out as previously described [25]. Quantification of the results was performed using Image J (National Institutes of Health, USA).

Staining of longissimus thoracis pectoralis section

For histological evaluation, Longissimus thoracis muscle was fixed in 4% paraformaldehyde and paraffin-embedded using standard procedures. The paraffin-embedded muscle was cut into 8 μm sections and stained with hematoxylin and eosin (H&E) using standard procedures.

To assess intramuscular fat content, 8 μm serial cryosections of muscle segments were prepared in a cryostat (Leica CM3050 S, Leica, Wetzlar, Germany) at -20˚C for Oil Red O staining.

Identification of longissimus thoracis muscle fiber type

To identify the fiber components of the longissimus thoracis, we sectioned the samples at 12 μm at -20℃. Sections were incubated overnight at 4 °C with a variety of primary antibodies for various fiber types: BA-D5 (for type I, 5 μg/mL, DSHB, USA), SC-71 (for type IIA, 5 μg/mL, DSHB, USA), and 10F5 (for type IIB, 5 μg/mL, DSHB, USA). After washing, the muscle segments were incubated for 4 h with isotype-specific secondary antibodies: Alexa Fluor 568-goat anti-mouse IgG2b cross-adsorbed secondary antibody (for BA-D5, 2 mg/mL, Invitrogen, USA), Alexa Fluor 488 goat anti-mouse IgG1 cross-adsorbed secondary antibody (SC-71, 2 mg/mL, Invitrogen, USA), and Alexa Fluor® 405 goat anti-mouse IgM (10F5, 1:2000, Abcam, USA). After washing, the muscle segments were gently coated with ProLong (Molecular Probes, Eugene, OR, USA) and covered with coverslips.

Statistical analysis

Data are expressed as mean ± SEM. Two-tailed, unpaired Student's t-tests were conducted to evaluate the data for analyzing intergroup differences between both groups. T-test was used to evaluate the comparative data between the two groups. $P < 0.05$ was regarded as statistically significant. GraphPad Prism version 8.0.2 (GraphPad Inc., La Jolla, CA, USA) was applied for the statistical analysis.

Results

Fat content was markedly higher in Laiwu pigs than in Yorkshire pigs

When compared at similar age (seven months) between two breeds, the body weight of Laiwu pigs was significantly lighter than that of Yorkshire pigs ($n = 6$) (Fig. 1A). Nevertheless, the average backfat thickness, percentage of fat (total, subcutaneous, perirenal, and mesenteric fat), the IMF content of Laiwu pigs were similar to those of Yorkshire pigs (Fig. 1B–E). Given the marked difference in body weight between the two pig breeds at similar age, and the impact of body weight difference on fat content, we next used the second cohort of pigs with similar body weight (approximately 110 kg) for the subsequently comparison. When comparing fat contents at a similar body weight (approximately 110 kg) between the two breeds (Fig. 1F), Laiwu pigs exhibited a two-fold higher average backfat thickness (Fig. 1G) and four-fold higher IMF content (Fig. 1H, I) compared to Yorkshire pigs. Laiwu pigs had a much greater fat percentage than Yorkshire pigs (Fig. 1J). Given these differences in fat content, pigs of similar body weights were selected for subsequent experiments.

Fat synthesis ability was more pronounced is Laiwu pigs than in Yorkshire pigs

To evaluate the effect of different fat contents in both pig breeds, we measured plasma levels of FFA, HDL, TG, and LDL in both breeds. Regarding lipid indicators, despite Laiwu pigs exhibiting a higher fat mass compared to Yorkshire (Fig. 1G–J), plasma FFA levels were significantly lower in Laiwu pigs than in Yorkshire (Fig. 2A). Furthermore, plasma TG levels were significantly lower in Laiwu pigs than in Yorkshire (Fig. 2B). Plasma LDL levels were comparable between the two breeds (Fig. 2C). However, plasma HDL levels were significantly higher in Laiwu pigs compared to Yorkshire (Fig. 2D), resulting in a lower LDL-to-HDL ratio in Laiwu pigs than in Yorkshire pigs (Fig. 2E). To elucidate the high fat content in Laiwu pigs, we assessed the markers of TG synthesis and degradation. Western blot analysis of key regulators of TG synthesis showed significantly elevated levels of ACC1, FASN, and PPARγ in adipose tissue of Laiwu pigs compared to Yorkshire pigs (Fig. 2F). Regarding TG degradation, the protein levels of HSL and ATGL, two major lipases involved in TG catabolism in adipose tissue, were similar between Laiwu and Yorkshire pigs (Fig. 2G). Taken together, these results suggest that the high fat content in Laiwu pigs may be attributed, at least in part, to elevated TG synthesis.

Laiwu pigs exhibit a high proportion of oxidative fibers in the longissimus thoracis

The IMF content in Laiwu pigs was greater than that in Yorkshire pigs. Statistical analysis and H&E staining of muscle fiber diameter and area exhibited that Laiwu pigs' longissimus thoracis fiber cross-sectional area was considerably smaller than that of Yorkshire pigs (Fig. 3A). Immunofluorescence staining of longissimus thoracis sections revealed a higher proportion of oxidized fibers in contrast to glycolytic fibers in Laiwu pigs than in Yorkshire pigs (Fig. 3B, Fig. S1A). RT-qPCR analysis demonstrated significantly higher expression levels of oxidized markers (MyHC I and MyHC IIA) in the longissimus thoracis of Laiwu pigs compared to Yorkshire pigs (Fig. 3C). As a result, Laiwu pigs had much lower glycolytic muscle fiber marker (MyHC IIB) expression levels than Yorkshire pigs (Fig. 3C). mRNA and protein levels of PGC1α, a crucial regulator of muscle fiber type transition, were

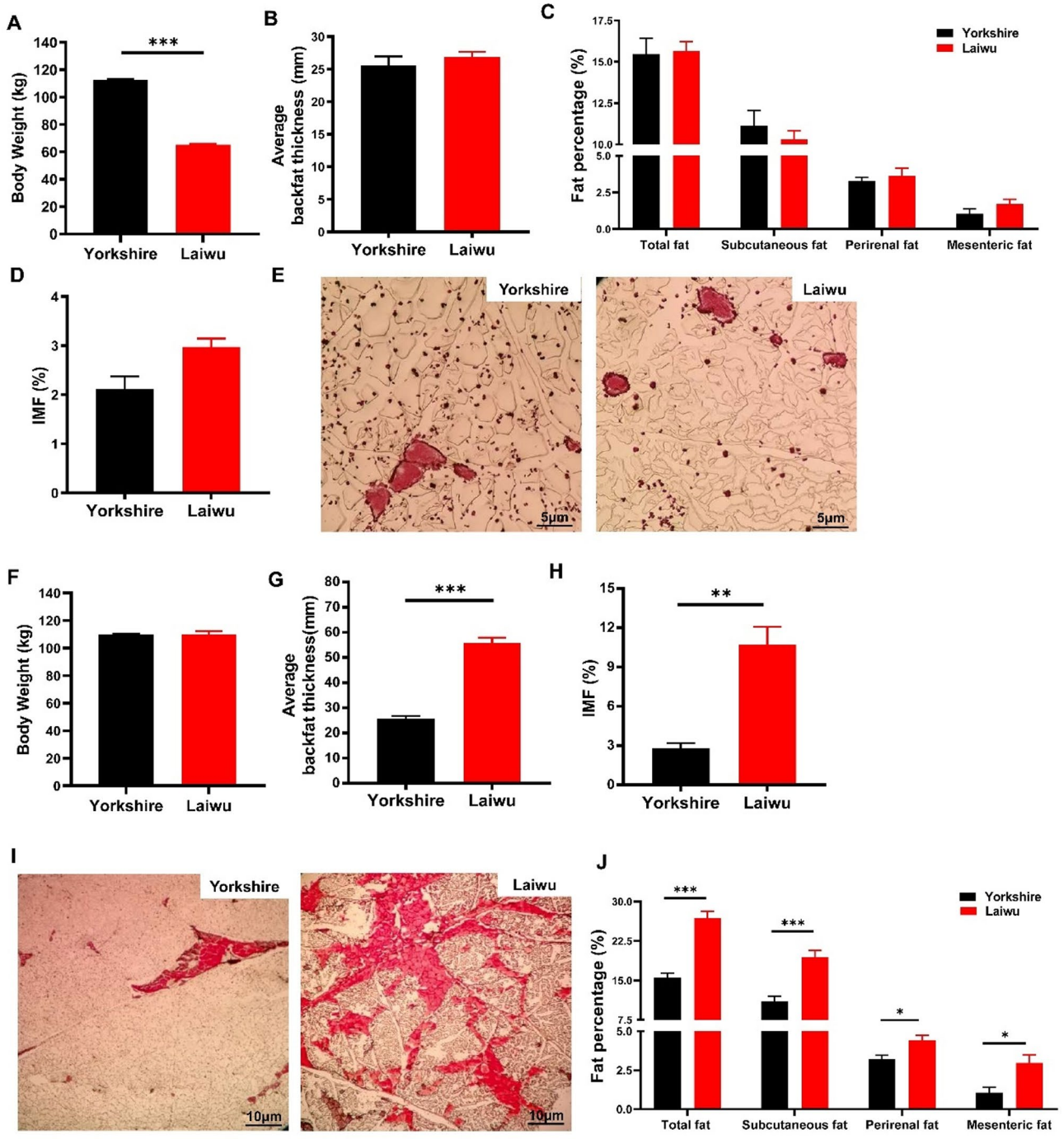

Fig. 1 The fat contents of Laiwu pig were significantly higher than those of Yorkshire pigs on the basis of similar body weight. Seven-month-old Yorkshire and Laiwu pigs were used for the following measurements (panel A-E, $n=6$): (**A**) Body weight. (**B**) Average backfat thickness. (**C**) Fat percentage. (**D**) Intramuscular fat percentage (Age-matched, $n=6$). (**E**) Oil Red O staining of longissimus thoracis. Similar body weight (around 110 kg) of Yorkshire and Laiwu pigs were used for the subsequent measurements: (**F**) Body weight. (**G**) Average backfat thickness. (**H**) Intramuscular fat percentage (Weight-matched, $n=6$). (**I**) Oil Red O staining of longissimus thoracis. (**J**) Fat percentage of different fat depots. Data were shown as means ± SEM. ($n=6$). *P* values were calculated by Two-tailed, unpaired Student's t-tests for comparisons. $^{*}P<0.05$, $^{**}P<0.01$, $^{***}P<0.001$

elevated in the longissimus thoracis of Laiwu pigs compared to Yorkshire pigs (Fig. 3D, E). Furthermore, mRNA levels of CD36, a fatty acid (FA) translocase, were higher in the longissimus thoracis of Laiwu pigs relative to Yorkshire pigs (Fig. 3F), indicating that Laiwu pigs had a greater IMF level than Yorkshire pigs. All of these findings point to a potential role for muscle fiber type in high IMF levels of Laiwu pigs.

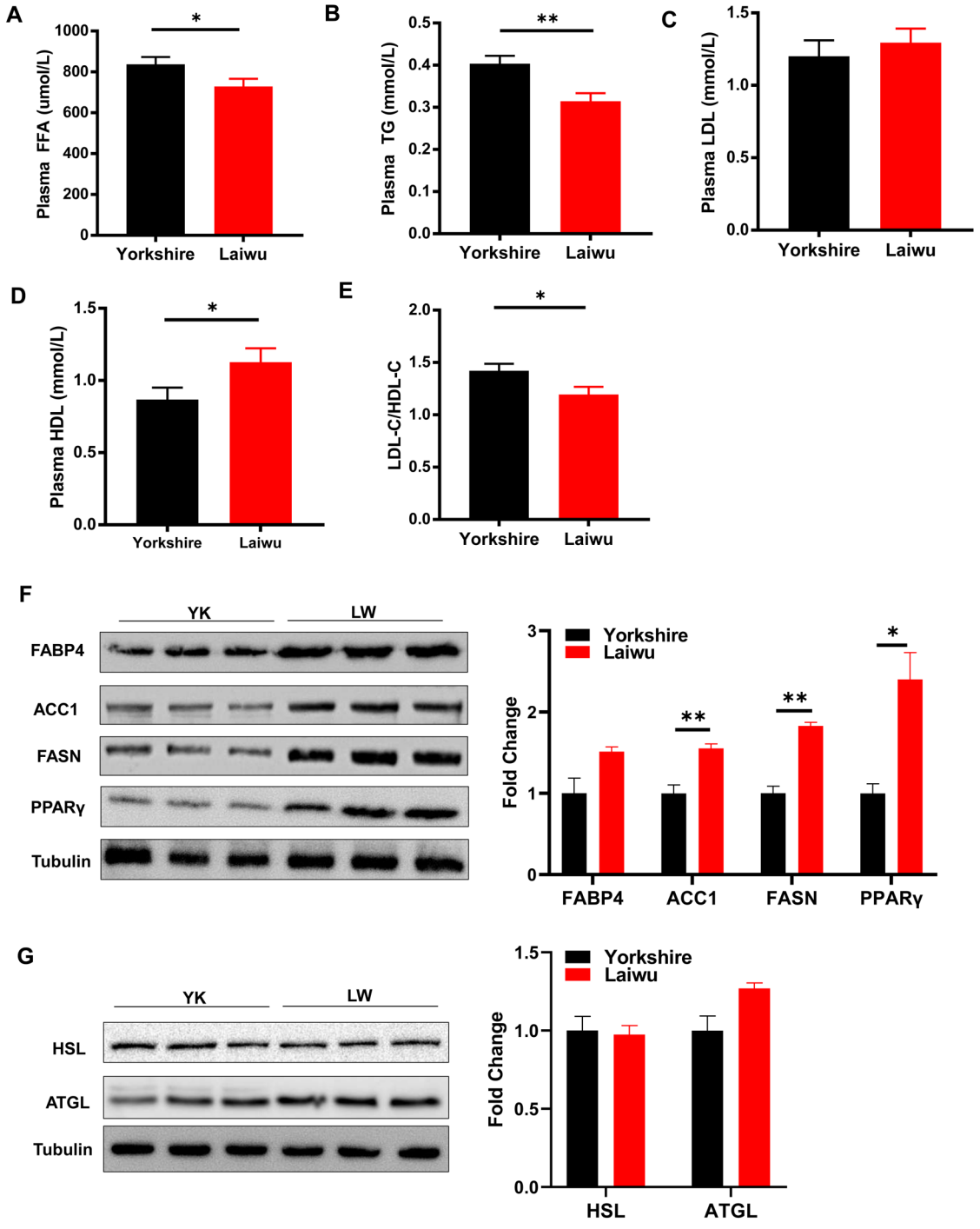

Fig. 2 Laiwu pigs show higher fat synthesis ability than Yorkshire pigs. (**A-D**) Plasma levels of FFA, TG, LDL and HDL($n=6$). (**E**) ratio of LDL to HDL($n=6$). Subcutaneous fat from 110 kg body weight 12 h-fasted Yorkshire and Laiwu pigs were used for the following measurements: (**F**) Expression levels of TAG synthesis-related proteins and protein quantification analysis ($n=3$). (**G**) Protein levels of two major adipose tissue lipases HSL&ATGL and protein quantification analysis ($n=3$). Data were shown as means ± SEM. *P* values were calculated by Two-tailed, unpaired Student's t-tests for comparisons. $^{*}P<0.05$, $^{**}P<0.01$, $^{***}P<0.001$. YK, Yorkshire pigs; LW, Laiwu pigs

Differences in skeletal muscle transcriptomics between Laiwu pigs and Yorkshire pigs

Transcriptomics analysis was conducted on Laiwu and Yorkshire pigs to examine gene expression patterns linked to IMF content in the longissimus thoracis. The analysis revealed 135 DEGs, including 56 downregulated and 79 upregulated genes in Laiwu pigs (Table 1). Figure 4A showed the distribution of DEGs. The disparities

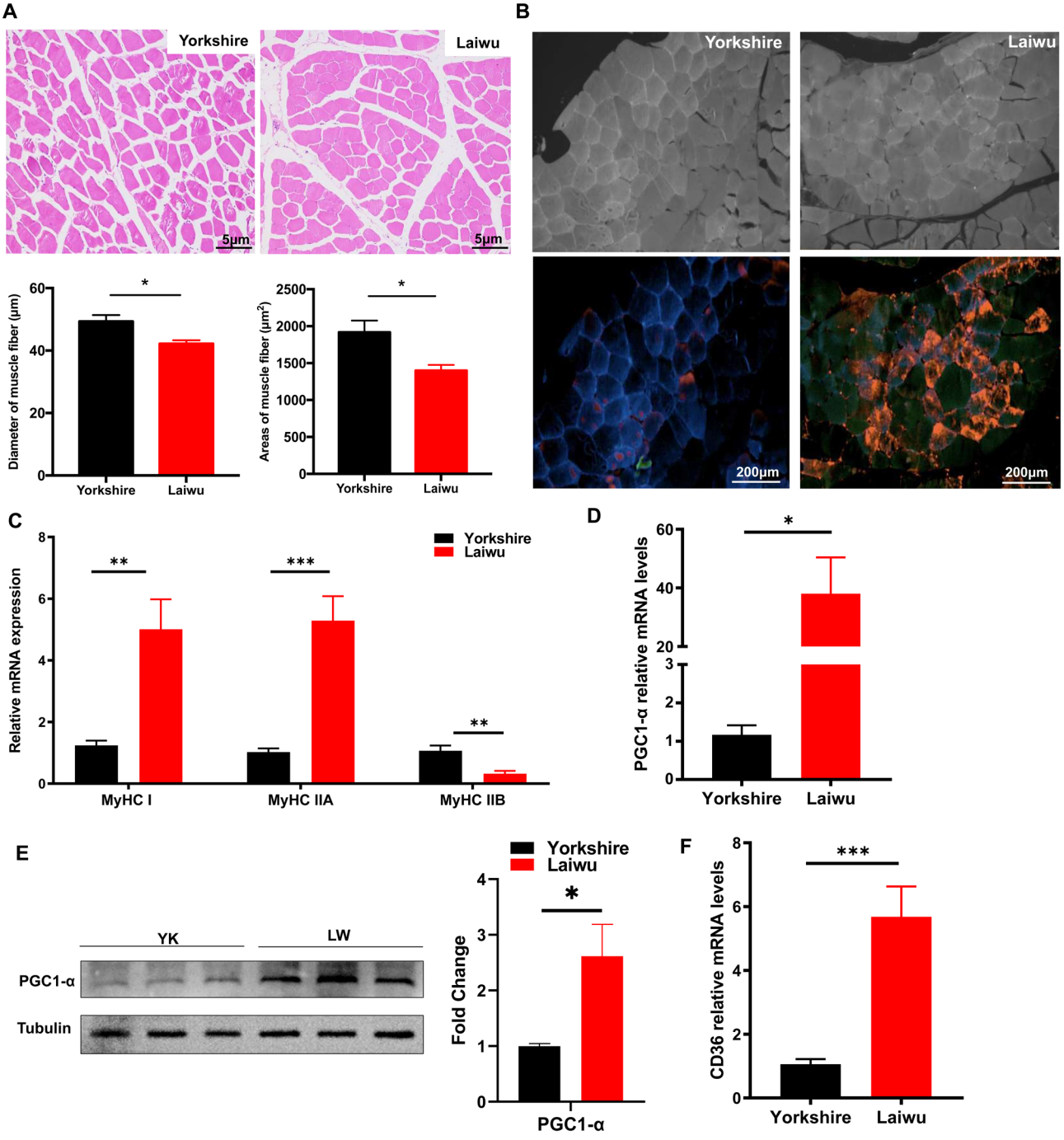

Fig. 3 Higher percentage of oxidized muscle fiber type in Laiwu pigs than in Yorkshire pigs. (**A**) H&E staining of longissimus thoracis. (**B**) longissimus thoracis fiber type immunofluorescence, type I fiber were shown in red, type IIA in green and type IIB in blue. The gray image represents the pre-staining control. (**C**) mRNA expression of fiber type-related genes from longissimus thoracis ($n=6$). (**D**) mRNA levels of PGC1α ($n=6$). (**E**) Levels of PGC1α protein and its quantification ($n=3$). (**F**) mRNA levels of CD36($n=6$). Data were shown as means ± SEM. *P* values were calculated by Two-tailed, unpaired Student's t-tests for comparisons. *$P<0.05$, **$P<0.01$, ***$P<0.001$. YK, Yorkshire pigs; LW, Laiwu pigs

in DEG expression patterns between Laiwu and Yorkshire pigs were graphically presented in the heat map (Fig. 4B). DEGs were categorized into 50 subcategories, including 25 biological processes (BPs), 15 cellular components (CCs) and 10 molecular functions (MFs) (Fig. 4C). The results exhibited a significant enrichment of terms mainly related to cellular anatomical entities, white adipocyte differentiation together with regulation of lipolytic processes ($P<0.05$) (Fig. 4D). We used the KEGG database to further explore the potential

Table 1 Significantly differential expression genes

Gene name	Regulation
FOXP2 GYS2 CCNB3 PPARG LEP TMEM25 KCNK3 SORL1	up
DAB1 RETSAT PLIN1	up
ADGRG2 MAL2 AOX1 CIDEC SDR16C5 SFRP1 LY49	up
ADIPOQ PROM1 LGALS12 TRARG1 COL12A1 ZSCAN23 DNAH14	up
SPATA18 PTGR1 CYP4B1 ACKR4 ITGAD PTCHD4	up
UNC93A PIF1 SFRP4 PPP1R1B PDE3B	up
MLXIPL NEGR1 CA5B STAR LOC102161686	up
IFN-ALPHA-15 ALDOC	up
ALDOC LAMB4 PIK3C2G FOXC2 FOXC2 PON3 LIPE CCDC65 PIEZO2	up
ALDH1L1 SEMA3D LRFN5	up
FFAR4 F5 ADIG	up
LOC100515685 MOB3B	up
HCAR1	up
GRIN3B SYNGR3 DGAT2 TLR7	up
FMOD KCNMB4	up
PDZD4 TWIST2 MATN4	up
KCNA3 COCH KLRK1	up
APOL6	up
LOC106504881	up
HCAR2 ACVR1C PLCH2	up
ENO4 LRRC24	up
Gene name	Regulation
CHRND SSPO ESRP1	down
CFAP97D1 POU2F2 TMEM151A SPP1	down
LYZ COL9A3 KCNMB1 OTOP3 FOXD1 CHRNE RAB38	down
ADAM28 LOC100624191	down
TBXAS1 UOX PADI2 SLC38A8	down
CHAC1 ADA2 SLC30A3 H2BC10 PRMT8	down
NTNG1	down
COL4A4 CD1E CRABP2	down
TNFSF9 SPAI-2	down
CD52 TIMP1 SCRG1 TENM2 HOXB5 LOC102158190 RAB20	down
ARSI THEM6 SUSD5 ZNHIT2 IRX1 NCAN	down
CTRC GPR162	down
SLC11A1 PCP4L1 NPHS2	down
PRSS56 GRIK3 LAG3 LRRC10B	down
FCRL3 CCR1	down
TYROBP	down

biological significance ($P < 0.05$). Based on the identified DEGs, the findings exhibited enrichment in many pathways, including the AMPK, cAMP and PPAR signaling pathways (Fig. 4E; Table 2). The PPAR signaling pathway, essential for lipid metabolism, shows enrichment of upregulated genes such as *PPARγ*, *PLIN1*, *ADIPOQ*, and *SCD* (Fig. 4F). Furthermore, the expression of four lipid metabolism-associated genes (*PPARγ*, *ADIPOQ*, *DGAT2*, and *SCD*) was validated among the DEGs listed using RT-qPCR, showing significant differences (Fig. 4G). The changes observed in RT-qPCR were consistent with those observed in RNA-seq. Based on the identified DEGs, the outcomes identified several enrichment pathways related to white adipocyte differentiation, lipid catabolism, and lipid metabolism, which likely contribute to factors influencing IMF in Laiwu pigs.

Abundance of lipid species in longissimus thoracis differs between Laiwu and Yorkshire pigs

To clarify the differences in lipid composition of muscle fat in Laiwu and Yorkshire pigs, we performed lipidomics analysis on the longissimus thoracis muscle, followed by data normalization. The PCA scores of the two breeds were shown in Fig. 5A. To further elucidate IMF-related molecular changes in Laiwu and Yorkshire pigs, we identified lipids exhibiting significant differences. The results were depicted in a volcano plot (Fig. 5B). A heatmap showed the content of different lipids (Fig. 5C). The biological pathways linked to lipid alterations were examined with the KEGG database (Fig. 5D). Lipolysis regulation, glycerolipid metabolism, and fat digestion and absorption in adipocytes, adipocytokine signaling pathway, and glycerophospholipid metabolism were among a few of the important lipid metabolism pathways that exhibited significant enrichment (Fig. 5E). The lipid composition was closely associated with phenotype. Consequently, lipid metabolism-related pathways in Laiwu and Yorkshire pigs were analyzed. Representative lipid species were distinguished using VIP scores. Among these candidate biomarkers, SHexCer 34:0;3O, SHexCer 41:5;3O, SHexCer 28:1, and TGs were upregulated in Laiwu pigs compared to Yorkshire pigs, whereas MG 16:0, MG 18:0, DG 18:0_18:0, and straight chain FAs were downregulated (Table 3). The discrepancies in IMF deposition between Laiwu and Yorkshire pigs might be attributed to these differential TGs and SHexCer.

Integrative transcriptomics and lipidomics analyses

To investigate the major genes and lipids influencing IMF content, we performed integrated transcriptomics and lipidomics analyses. Key pathways affecting IMF content were further identified using the KEGG database. As shown in Fig. 6A, the Venn diagram illustrated KEGG pathways implicated in transcriptomics and lipidomics, with 20 pathways showing overlap between the two omics studies. By integrating transcriptomics and lipidomics data, we annotated several important pathways with DEGs and differentially expressed lipids (Fig. 6B). Significant DEGs were presented in Fig. 6C. This included 35 downregulated and 57 upregulated genes out of a total of 92 DEGs (Table 4). This analysis underscored the pathways associated with lipid metabolism. Furthermore, we found that the fat digestion and absorption pathway exhibited 39 differential lipids (2 MGs, 3 CEs, 2 FAs, and 32 TGs) that were significantly altered between Laiwu and Yorkshire pigs (Fig. 6D; Table 5). Specifically, the

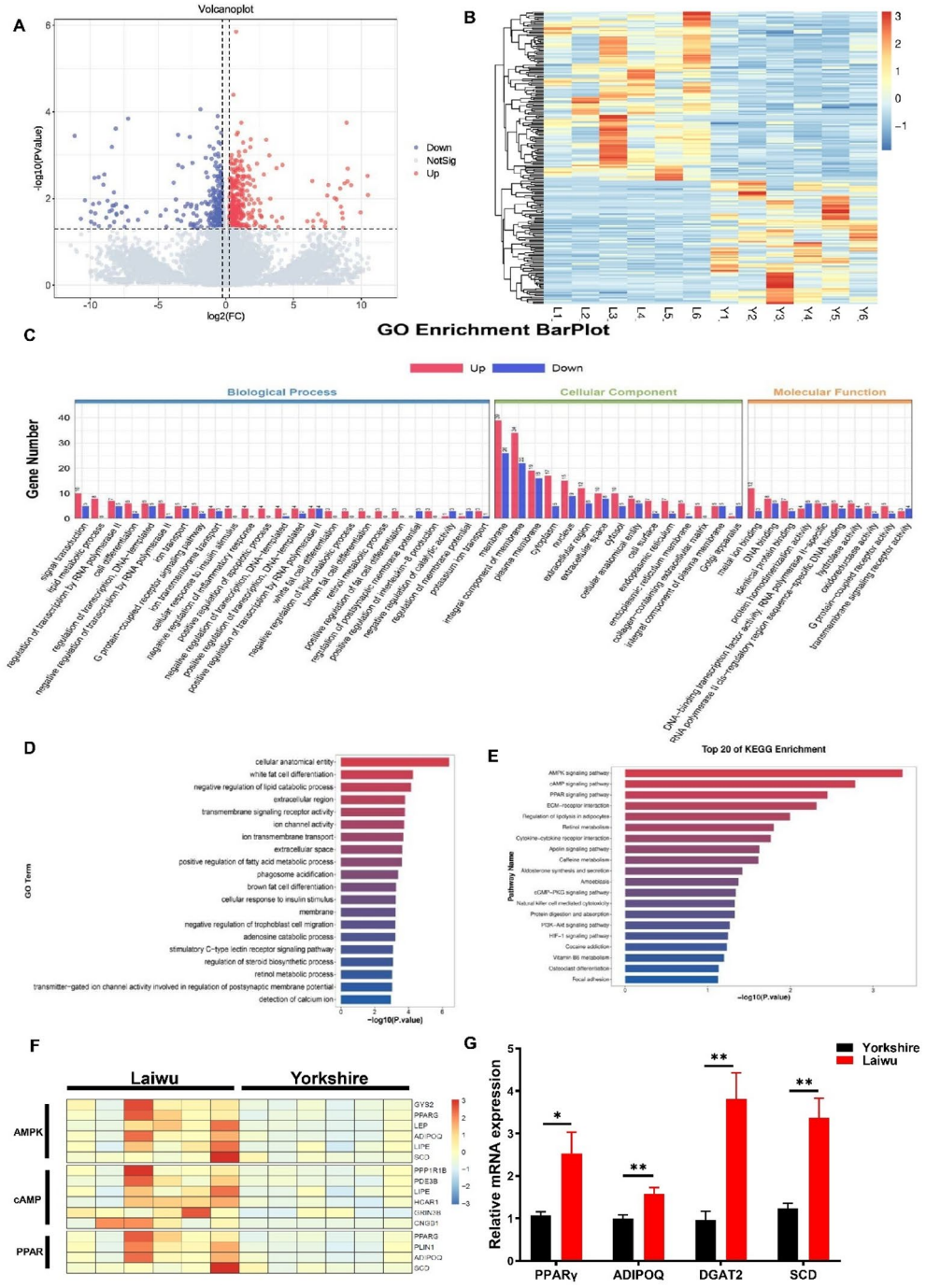

Fig. 4 Skeletal muscle transcriptomic data analysis in pigs. Longissimus thoracis from 6 Yorkshire and 6 Laiwu pigs were used for the following measurements. (**A**) Volcano plot for screening of DEGs. The blue dots represent the downregulated expressed genes; the red dots represent the upregulated expressed genes; the black dots represent the non-differentially expressed genes. The abscissa indicates the differential expression multiple; the ordinate indicates the difference significance in the gene. (**B**) Cluster heat map of DEGs. L1-L6, Laiwu pigs; Y1-6, Yorkshire pigs. (**C-D**) The column diagrams for GO annotation analysis of DEGs. The abscissa indicates the functions of GO analysis; the ordinate indicates the numbers of DEGs annotated. (**E**) The diagrams for the KEGG pathway enrichment of DEGs. The abscissa indicates the value of rich factors (the ratio of annotated DEGs to all genes of the enriched pathway); the ordinate indicates the pathways enriched. *P*-value of each term is represented by the color. (**F**) Pre-three enrichment pathway. (**G**) Expression levels of candidate DEGs (PPARγ, ADIPOQ, DGAT2 and SCD) assessed by RT-qPCR. Data were shown as means ± SEM. *P* values were calculated by Two-tailed, unpaired Student's t-tests for comparisons. **P* < 0.05, ***P* < 0.01, ****P* < 0.001. YK, Yorkshire pigs; LW, Laiwu pigs

Table 2 Enrichment of DEGs signaling pathways

Term	Category	*P*.value	Up	Down
Cellular anatomical entity	Cellular Component	3.92E-07	MAL2, PROM1, COL12A1, UNC93A, GRIN3B, MATN4, KCNA3	CHRND, CHRNE, NTNG1, COL4A4, NCAN, GRIK3
White fat cell differentiation	Biological Process	5.46698E-05	PPARG, ADIG, FFAR4	
Negative regulation of lipid catabolic process	Biological Process	7.07368E-05	PLIN1, PDE3B, HCAR1	
Extracellular region	Cellular Component	0.000162503	LEP, SORL1, SFRP1, ADIPOQ, COL12A1, SFRP4, IFN-ALPHA-15, SEMA3D, F5, FMOD, ADAMTS18	SPP1, ADA2, SPAI-2, TIMP1, NCAN, LAG3
Transmembrane signaling receptor activity	Molecular Function	0.000165819	SORL1, ADGRG2, TLR7	CHRND, CHRNE, LAG3, FCRL3
Ion channel activity	Molecular Function	0.000177499	KCNK3, GRIN3B, KCNA3	CHRND, CHRNE, GRIK3
Ion transmembrane transport	Biological Process	0.000202856	KCNK3, PIEZO2, GRIN3B, KCNA3	CHRND, CHRNE, GRIK3
Extracellular space	Cellular Component	0.000231101	LEP, SORL1, SFRP1, ADIPOQ, COL12A1, SFRP4, IFN-ALPHA-15, PON3, F5, LRRC24	LYZ, SPP1, COL9A3, ADA2, CD1E, SPAI-2, TIMP1, PRSS56
Positive regulation of fatty acid metabolic process	Biological Process	0.000243714	PPARG, ADIPOQ	
Phagosome acidification	Biological Process	0.000404477		RAB38, RAB20
Brown fat cell differentiation	Biological Process	0.000537653	ADIPOQ, ADIG, FFAR4	
Cellular response to insulin stimulus	Biological Process	0.0005638	PPARG, LEP, ADIPOQ, TRARG1	
Membrane	Cellular Component	0.000577474	TMEM25, KCNK3, SORL1, ADGRG2, MAL2, PROM1, TRARG1, SPATA18, CYP4B1, ACKR4, ITGAD, PTCHD4, UNC93A, PPP1R1B, PDE3B, LAMB4, PIK3C2G, LIPE, PIEZO2, SEMA3D, LRFN5, ADIG, FFAR4, HCAR1, TLR7, DGAT2, SYNGR3, GRIN3B, KCNMB4, KLRK1, KCNA3, LRRC24, ACVR1C, SCD	CHRND, TMEM151A, KCNMB1, OTOP3, CHRNE, RAB38, ADAM28, TBXAS1, SLC38A8, SLC30A3, NTNG1, COL4A4, CD1E, TNFSF9, CD52, TENM2, RAB20, SUSD5, GPR162, TYROBP, SLC11A1, NPHS2, GRIK3, LAG3, FCRL3, CCR1
Adenosine catabolic process	Biological Process	0.000604159		UOX, ADA2
Negative regulation of trophoblast cell migration	Biological Process	0.000604159	ACVR1C	TIMP1
Regulation of steroid biosynthetic process	Biological Process	0.000842261	LEP, STAR	
Stimulatory C-type lectin receptor signaling pathway	Biological Process	0.000842261	KLRK1	TYROBP
Transmitter-gated ion channel activity involved in regulation of postsynaptic membrane potential	Molecular Function	0.000927074		CHRND, CHRNE, GRIK3
Retinol metabolic process	Biological Process	0.000927074	RETSAT, SDR16C5, LIPE	
Detection of calcium ion	Biological Process	0.001118288	KCNMB4	KCNMB1

abundance of some short-chain and medium-chain TGs was significantly higher in Laiwu pigs, whereas some long-chain TGs were more abundant in Yorkshire pigs. The interworking network showed the status of interactions involving KEGG pathways, notably identifying co-metabolites such as FAs within these pathways (Fig. 6E). Among them, TGs and 1-acylglycerol exhibited overlap in pathways associated with fat digestion and absorption, together with the modulation of lipolysis in fat cells. As depicted in Fig. 7, the synthesis pathway of lipid metabolites elucidated the roles of significantly different genes within the lipid synthesis pathway, shedding light on the high-level regulatory processes governing IMF in Laiwu pigs. The gene expression changes verified through RT-qPCR are consistent with those presented in Fig. 7 (Fig. S1B). Additionally, the TG content in the longissimus thoracis muscle of Laiwu pigs was significantly higher than that of Yorkshire pigs, which was also in agreement with the findings shown in Fig. 7 (Fig. S1C). This reinforces the validity of our screened candidate genes.

Discussion

The IMF serves as a key indicator of meat quality, providing guidance on pork market management and breeding programs. In this study, transcriptomics and lipidomics analyses were performed to explore the complex biological processes affecting IMF deposition. Our analysis focused specifically on biological processes exhibiting significant differences between the two breeds Laiwu and Yorkshire pig. The results may contribute to guiding the

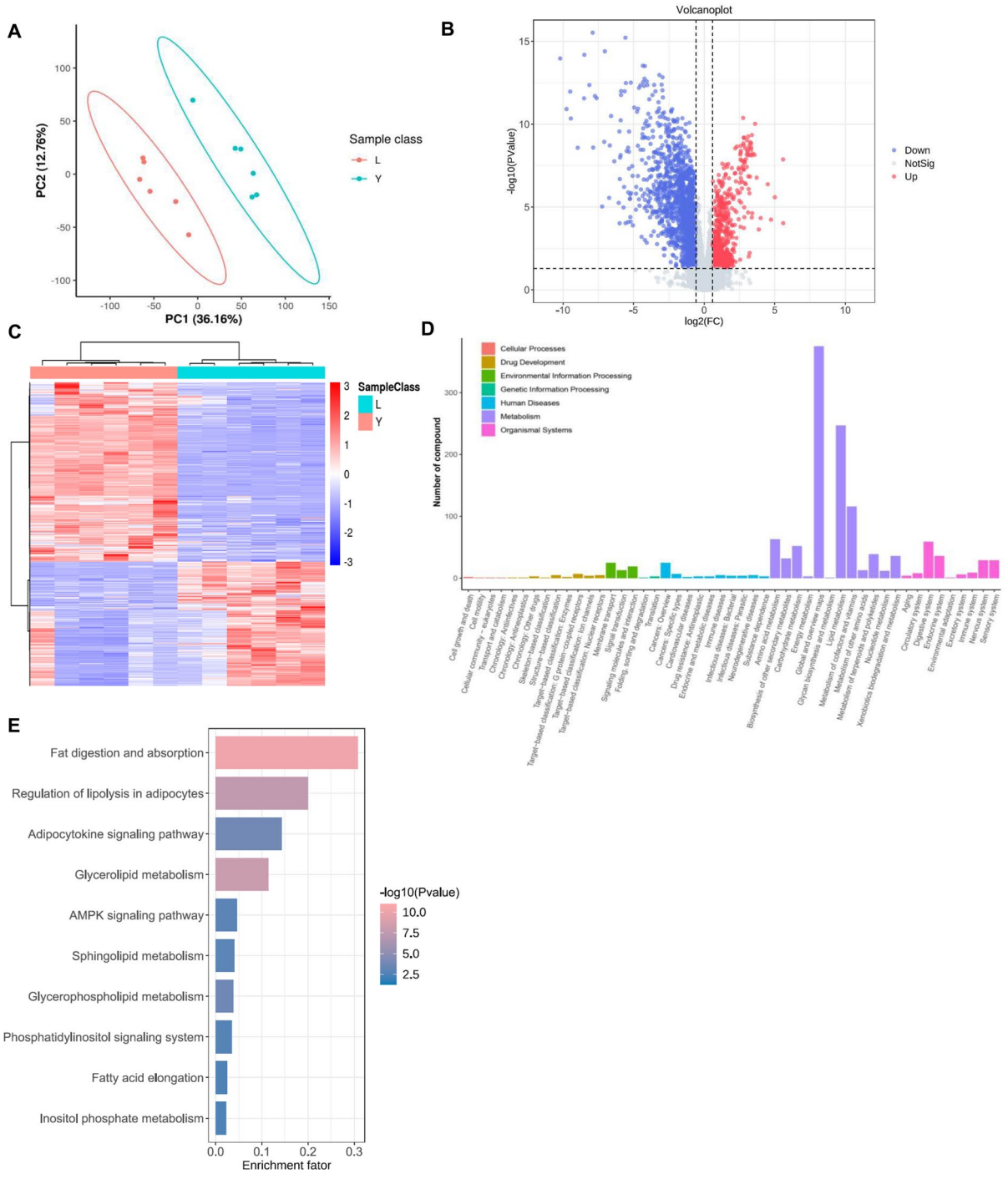

Fig. 5 Longissimus Thoracis lipidomic profiling in pigs Longissimus thoracis from 6 Yorkshire and 6 Laiwu pigs were used for lipidomics analysis. (**A**) Principal component analysis (PCA). (**B**) Volcano plots of differentially expressed lipids. In the volcano plot, red represents upregulated lipids, and blue represents downregulated lipids, gray represents a lipid with no differential expression. (**C**) Cluster heat map of differentially expressed lipids. (**D-E**) The diagrams for the KEGG pathway enrichment degree of differentially expressed lipids

improvement of pork quality at the genetic and molecular levels. Unlike previous studies, this research used adult pigs of similar body weight instead of similar age. Although Yorkshire pigs reach approximately 110 kg at 7 months of age, Laiwu pigs require 9 to 10 months to attain the same weight. Previous studies have shown that in Chinese native breeds, there are no significant differences in fatty acid, amino acid and metabolites between 210 and 300 days of age [26].This suggests that changes in fatty acid, amino acid and metabolites profiles after

Table 3 Significant differences in lipids

ID	*P*.value	VIP	Regulated	
MG 18:0	1.74E-05	3.229448347	down	Monoacylglycerols
DG 18:0_18:0	4.74E-09	3.116783954	down	Diacylglycerols
MG 16:0	3.04E-06	3.110879719	down	Monoacylglycerols
DG 16:0_18:0	4.27E-05	2.343161373	down	Diacylglycerols
CE 18:2	0.011988583	2.270749412	down	Sterol esters
DG 18:0_20:0	1.51E-06	2.265949604	down	Diacylglycerols
CE 20:4	0.033838341	2.028160731	down	Sterol esters
DG 16:0_16:0	1.60E-05	1.915088858	down	Diacylglycerols
FA18: 2	0.002944506	1.749480026	down	Straight chain fatty acids
CE 22:6	0.014857255	1.609977721	down	Sterol esters
TG 15:0_19:1_20:1	0.024763461	1.386355854	down	Triacylglycerols
TG 18:0_18:0_18:0	0.031275271	1.351845587	down	Triacylglycerols
TG 16:0_16:0_18:1	0.013786431	1.344092423	down	Triacylglycerols
FA 20:2	0.004470289	1.302672949	down	Straight chain fatty acids
CL 36:3_36:4	0.031946587	1.264785515	down	Diacylglycerophosphoglycerophosphodiradylglycerols
TG 16:1_18:0_18:0	0.004645961	1.14988788	down	Triacylglycerols
TG 17:0_18:1_18:1	0.036178985	1.129614072	down	Triacylglycerols
SHexCer 34:0;3O	5.20E-06	2.383210391	up	Sulfoglycosphingolipids (sulfatides)
SHexCer 41:5;3O	0.000456302	2.325288802	up	Sulfoglycosphingolipids (sulfatides)
TG 8:0_18:1_18:2	0.012244101	1.999679593	up	Triacylglycerols
TG 8:0_16:1_18:1	0.020271672	1.963874318	up	Triacylglycerols
TG 10:0_18:1_18:2	0.015378418	1.918103009	up	Triacylglycerols
TG 10:0_16:1_18:1	0.018584169	1.889491809	up	Triacylglycerols
TG 8:0_16:0_18:1	0.021905599	1.876847793	up	Triacylglycerols
TG 10:0_10:0_18:1	0.031380328	1.8340023	up	Triacylglycerols
TG 14:0_16:0_18:0	0.025163061	1.829741225	up	Triacylglycerols
TG 14:1_16:1_18:1	0.013556752	1.826436757	up	Triacylglycerols
TG 10:0_18:1_18:1	0.025359275	1.797341072	up	Triacylglycerols
TG 10:0_16:0_18:1	0.028934104	1.777227393	up	Triacylglycerols
TG 10:0_16:0_16:0	0.043339834	1.727128362	up	Triacylglycerols
TG 8:0_16:1_18:1	0.022320221	1.716938195	up	Triacylglycerols
TG 10:0_18:0_18:1	0.019219151	1.675726251	up	Triacylglycerols
TG 10:0_18:0_18:1	0.029528147	1.662400909	up	Triacylglycerols
TG 16:1_17:1_18:2	0.011411731	1.620120992	up	Triacylglycerols
TG 16:1_16:1_18:1	0.017731465	1.547171692	up	Triacylglycerols
TG 10:0_17:1_18:1	0.016038929	1.546749435	up	Triacylglycerols
TG 14:0_16:1_18:1	0.02641014	1.527016704	up	Triacylglycerols
TG 8:0_17:1_18:1	0.013807251	1.521421181	up	Triacylglycerols
TG 9:0_16:0_18:1	0.018229196	1.431138509	up	Triacylglycerols
TG 13:0_17:1_19:1	0.020732038	1.415061511	up	Triacylglycerols
TG 16:1_17:1_18:1	0.015877852	1.41299442	up	Triacylglycerols
TG 8:0_10:0_18:1	0.004977594	1.390361063	up	Triacylglycerols
TG 10:0_17:0_18:1	0.037398913	1.372819517	up	Triacylglycerols
TG 11:0_17:1_19:1	0.033745552	1.337722194	up	Triacylglycerols
TG 8:0_16:1_18:1	0.024761414	1.21964473	up	Triacylglycerols
TG 17:1_18:1_18:2	0.04041479	1.206056114	up	Triacylglycerols
SHexCer 28:1	0.03729724	1.11728132	up	Sulfoglycosphingolipids (sulfatides)

reaching adulthood are relatively small, with less pronounced variations compared to the growth period. Therefore, by using pigs of similar body weight, we minimized age-related effects, enabling a more accurate comparison between the two breeds. This enables a more precise assessment of the differences in IMF content between Laiwu and Yorkshire pigs, while the combined analysis of transcriptomics and lipidomics enhances the identification of gene-lipid interactions and their regulatory pathways.

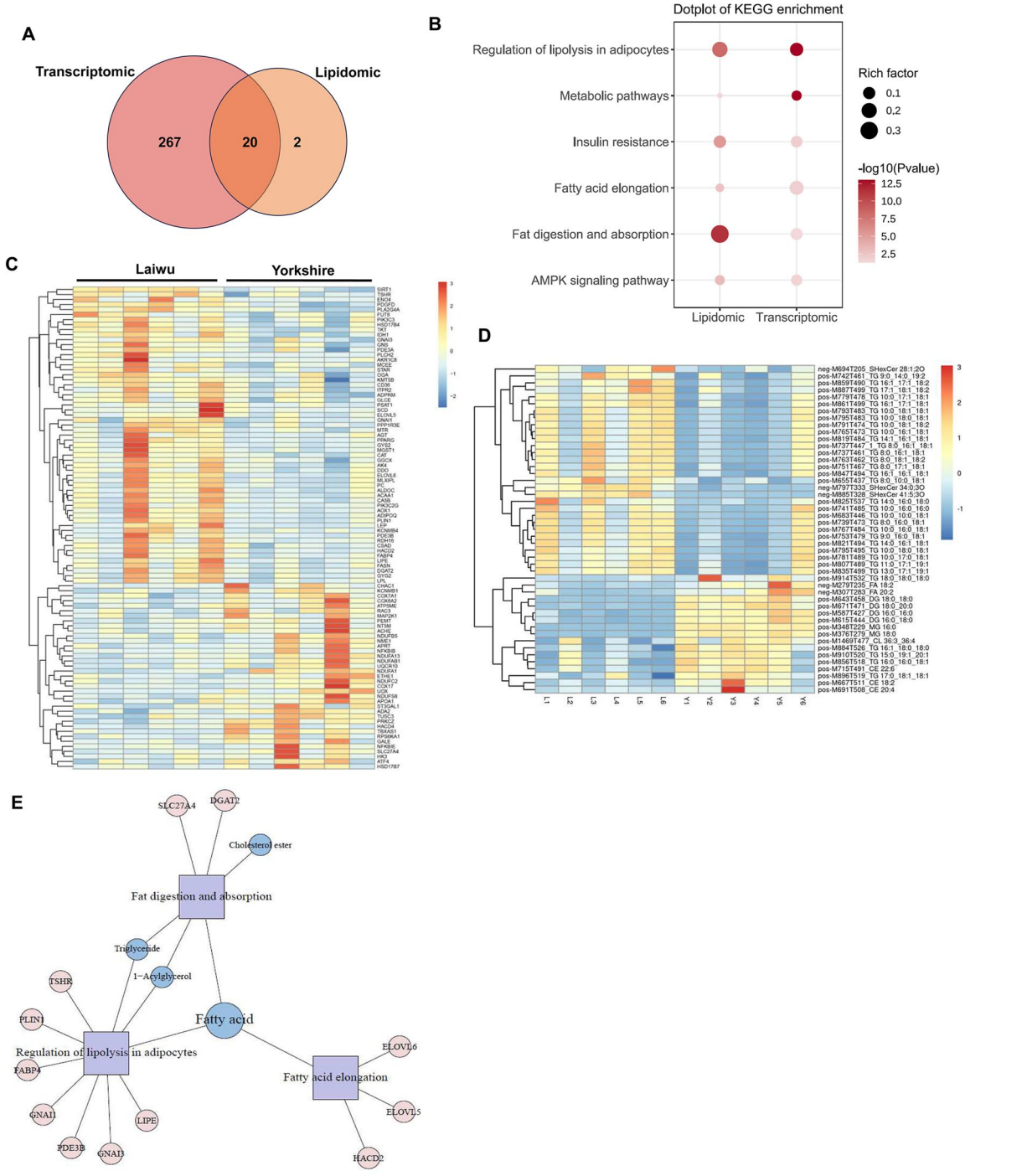

Fig. 6 Integrative analysis of transcriptomic and lipidomic. (**A**) Venn diagram of KEGG enrichment pathways based on transcriptomic and lipidomic. (**B**) Shared pathways of transcriptomic and lipidomic based on KEGG enrichment. (**C**) Significant DEGs based on transcriptomic and lipidomic. (**D**) Significant differential metabolites based on transcriptomic and lipidomic. (**E**) Interworking network of transcriptomic and lipidomic by combined analysis

Notably, when comparing pigs of the same body weight, Laiwu pigs demonstrated a substantially higher IMF content, a finding consistent with previous studies [27]. Research has shown that the meat quality of the longissimus dorsi muscle in Laiwu pigs differs from Duroc × Landrace × Yorkshire pigs [8]. Zheng et al. [28]. showed that type IIA fibers had intermediate levels of myoglobin, whereas type I myofibers had about four times the amount. According to previous studies, there is a positive correlation between the proportion of oxidized fibers and tenderness [29–31]. Muscles predominantly composed of red fibers generally exhibit high IMF content

Table 4 Differentially expressed genes through integrated transcriptomic and lipidomic analysis

Gene name	Laiwu pig (Average expression values)	Yorkshire pig (Average expression values)	Fold Change	Description
GYS2	0.45	0.12	3.6	glycogen synthase 2
PPARG	2.06	0.85	2.42	peroxisome proliferator activated receptor gamma
LEP	0.37	0.11	3.5	leptin
ADIPOQ	37.11	11.50	3.23	adiponectin, C1Q and collagen domain containing
SIRT1	3.15	2.58	1.22	sirtuin 1
LIPE	5.98	2.96	2.02	lipase E, hormone sensitive type
FASN	21.44	11.25	1.91	fatty acid synthase
CD36	36.70	28.26	1.3	CD36 molecule
SCD	12.53	5.29	2.37	stearoyl-CoA desaturase
PIK3C2G	0.16	0.03	5.23	phosphatidylinositol-4-phosphate 3-kinase catalytic subunit type 2 gamma
PIK3C3	1.91	1.46	1.3	phosphatidylinositol 3-kinase catalytic subunit type 3
ITPR2	1.77	1.27	1.4	inositol 1,4,5-trisphosphate receptor type 2
PDGFD	2.72	2.08	1.3	platelet derived growth factor D
PLA2G4A	0.40	0.22	1.8	phospholipase A2 group IVA
RAC3	5.28	6.97	0.76	Rac family small GTPase 3
MAP2K1	11.35	14.74	0.77	mitogen-activated protein kinase kinase 1
PRKCZ	0.16	0.23	0.69	protein kinase C zeta
MLXIPL	1.74	0.82	2.13	MLX interacting protein like
RPS6KA1	0.27	0.45	0.59	ribosomal protein S6 kinase A1
AGT	10.70	5.86	1.83	angiotensinogen
SLC27A4	0.65	0.84	0.77	solute carrier family 27member 4
PPP1R3E	1.42	0.96	1.48	protein phosphatase 1 regulatory subunit 3E
OGA	30.09	24.83	1.21	O-GlcNAcase
NDUFAB1	12.08	14.87	0.81	NADH: ubiquinone oxidoreductase subunit AB1
NDUFA1	7.72	10.65	0.73	NADH: ubiquinone oxidoreductase subunit A1
COX6A2	26.99	34.96	0.77	cytochrome c oxidase subunit 6A2
NDUFS6	25.58	32.05	0.8	NADH: ubiquinone oxidoreductase subunit S6
COX7A1	6.14	7.40	0.83	cytochrome c oxidase subunit 7A1
UQCR10	23.95	29.14	0.82	ubiquinol-cytochrome c reductase, complex III subunit X
NDUFC2	3.78	4.76	0.79	NADH: ubiquinone oxidoreductase subunit C2
NDUFB5	5.54	6.85	0.81	NADH: ubiquinone oxidoreductase subunit B5
NDUFA13	6.46	8.01	0.81	NADH: ubiquinone oxidoreductase subunit A13
ATF4	1667.11	2038.23	0.82	activating transcription factor 4
HK3	0.73	1.28	0.57	hexokinase 3
HACD2	2.55	1.38	1.94	3-hydroxyacyl-CoA dehydratase 2
MGST1	2.17	1.12	2	microsomal glutathione S-transferase 1
AOX1	1.86	0.93	1.82	aldehyde oxidase 1
ELOVL6	2.13	1.17	1.35	ELOVL fatty acid elongase 6
TKT	6.25	4.61	1.62	transketolase
ACAA1	3.64	2.25	0.53	acetyl-CoA acyltransferase 1
NME1	0.68	1.30	2.43	NME/NM23 nucleoside diphosphate kinase 1
PDE3B	0.53	0.22	1.8	phosphodiesterase 3B
AK4	2.24	1.25	2.4	adenylate kinase 4
CA5B	1.14	0.47	1.51	carbonic anhydrase 5B
PC	28.84	19.14	2.59	pyruvate carboxylase
ALDOC	6.99	2.70	1.4	aldolase, fructose-bisphosphate C
MTR	2.80	2.00	1.21	5-methyltetrahydrofolate-homocysteine methyltransferase
CHAC1	0.54	1.86	1.4	ChaC glutathione specific gamma-glutamylcyclotransferase 1
ADA2	0.10	0.26	1.26	adenosine deaminase 2
MCEE	3.45	2.84	0.56	methylmalonyl-CoA epimerase
IDH1	6.84	4.88	2.43	isocitrate dehydrogenase (NADP (+)) 1

Table 4 (continued)

Gene name	Laiwu pig (Average expression values)	Yorkshire pig (Average expression values)	Fold Change	Description
HSD17B4	13.17	10.44	1.31	hydroxysteroid 17-beta dehydrogenase 4
HSD17B7	0.74	1.31	0.73	hydroxysteroid 17-beta dehydrogenase 7
DGAT2	4.50	1.85	1.28	diacylglycerol O-acyltransferase 2
CAT	39.33	30.02	1.2	catalase
APRT	2.80	3.82	1.56	adenine phosphoribosyltransferase
ADPRM	1.01	0.79	1.54	ADP-ribose/CDP-alcohol diphosphatase, manganese dependent
GNS	14.36	11.96	1.25	glucosamine (N-acetyl)-6-sulfatase
GYG2	0.92	0.59	0.54	glycogenin 2
DDO	3.37	2.19	1.51	D-aspartate oxidase
GGCX	4.72	3.77	0.7	gamma-glutamyl carboxylase
HACD4	0.11	0.21	0.71	3-hydroxyacyl-CoA dehydratase 4
ELOVL5	4.66	3.07	0.72	ELOVL fatty acid elongase 5
NT5M	2.94	4.19	0.75	5',3'-nucleotidase, mitochondrial
ATP5ME	1.08	1.52	0.71	ATP synthase membrane subunit e
GALE	1.30	1.80	1.63	UDP-galactose-4-epimerase
ST3GAL1	2.27	3.04	0.79	ST3 beta-galactoside alpha-2,3-sialyltransferase 1
TUSC3	0.45	0.63	0.73	tumor suppressor candidate 3
AKR1C8	19.71	12.11	1.3	aldo-keto reductase family 1 member C4
COX17	33.49	42.40	3.6	cytochrome c oxidase copper chaperone COX17
PEMT	8.46	11.60	2.42	phosphatidylethanolamine N-methyltransferase
FUT8	4.42	3.40	3.5	fucosyltransferase 8
GLCE	1.42	1.12	1.27	glucuronic acid epimerase
PSAT1	3.15	1.97	1.6	phosphoserine aminotransferase 1
ETHE1	1.56	2.08	0.75	ETHE1 persulfide dioxygenase
PDE3A	0.78	0.57	1.36	phosphodiesterase 3 A
KMT5B	7.09	5.80	1.22	lysine methyltransferase 5B
RDH16	2.51	1.61	1.56	retinol dehydrogenase 16 (all-trans)
CSAD	0.82	0.52	1.56	cysteine sulfinic acid decarboxylase
LPL	36.24	21.82	1.66	lipoprotein lipase
ACHE	0.51	0.99	0.51	acetylcholinesterase
APOA1	4.04	5.70	0.71	apolipoprotein A1
PLIN1	12.49	3.95	3.16	perilipin 1
FABP4	25.79	16.02	1.61	fatty acid binding protein 4, adipocyte
GNAI1	2.57	1.78	1.44	G protein subunit alpha i1
TSHR	1.09	0.79	1.38	thyroid stimulating hormone receptor
GNAI3	1.61	1.33	1.22	G protein subunit alpha i3
NFKBIB	3.23	4.39	0.73	NFKB inhibitor beta
NFKBIE	1.01	1.43	0.7	NFKB inhibitor epsilon
KCNMB1	0.12	0.34	0.37	potassium calcium-activated channel subfamily M regulatory beta subunit 1
KCNMB4	0.13	0.05	2.54	potassium calcium-activated channel subfamily M regulatory beta subunit 4
STAR	0.24	0.12	2.02	steroidogenic acute regulatory protein

[31], which in turn positively correlates with tenderness [32]. Additionally, small muscle fibers tend to correlate with increased tenderness, with type I fibers typically being small [33, 34]. Laiwu pigs showed higher mRNA levels of MyHC IIA and MyHC I than lean pig breeds, but lower MyHC IIB expression levels. Consistent with this observation, in comparison with Yorkshire pigs, we found a higher proportion of oxidized fiber types in the longissimus thoracis of Laiwu pigs, as evidenced by (1) immunofluorescence staining and (2) elevated expression of PGC1α, a marker of oxidized fiber types, in the longissimus thoracis of Laiwu pigs versus Yorkshire pigs. We therefore reasoned that the IMF content in Laiwu pigs may be influenced by the muscle fiber type composition.

Previous studies have demonstrated a correlation between the IMF content of pigs and the enzymes and

Table 5 Differentiation of lipid profiles through integrated transcriptomic and lipidomic analysis

Metabolite	Laiwu pig (Average expression values)	Yorkshire pig (Average expression values)	*P*.value
TG 8:0_10:0_18:1	14665.29263	8354.618024	4.98E-03
TG 10:0_10:0_18:1	76080.55284	33860.16278	3.14E-02
TG 8:0_16:1_18:1	14381.75174	6949.891891	2.03E-02
TG 8:0_16:0_18:1	1141090.792	506047.0279	2.19E-02
TG 10:0_16:0_16:0	792900.582	406749.9783	4.33E-02
TG 9:0_14:0_19:2	16479.48989	10921.07488	2.48E-02
TG 8:0_17:1_18:1	17920.15847	10140.47538	1.38E-02
TG 9:0_16:0_18:1	36579.51496	22359.2926	1.82E-02
TG 8:0_18:1_18:2	263902.2993	101523.1144	1.22E-02
TG 10:0_16:1_18:1	2920705.157	1248224.051	1.86E-02
TG 10:0_16:0_18:1	4900778.887	2335224.532	2.89E-02
TG 10:0_17:1_18:1	88107.40886	48978.90325	1.60E-02
TG 10:0_17:0_18:1	97128.00138	62370.11681	3.74E-02
TG 10:0_18:1_18:2	1831274.158	752827.3306	1.54E-02
TG 10:0_18:1_18:1	9616470.535	4436366.085	2.54E-02
TG 10:0_18:0_18:1	1370605.35	702023.2009	2.95E-02
TG 11:0_17:1_19:1	145513.3225	94018.91641	3.37E-02
TG 14:1_16:1_18:1	2354251.729	1073748.166	1.36E-02
TG 14:0_16:1_18:1	11217768.31	6387369.325	2.64E-02
TG 14:0_16:0_18:0	187649.2938	67749.87069	2.52E-02
TG 13:0_17:1_19:1	496398.7603	308347.4805	2.07E-02
TG 16:1_16:1_18:1	16319677.01	9113738.464	1.77E-02
TG 16:1_17:1_18:2	126278.3259	63864.6065	1.14E-02
TG 16:1_17:1_18:1	810327.7621	493420.7702	1.59E-02
TG 17:1_18:1_18:2	395149.0098	254337.3915	4.04E-02

genes that control lipid metabolism and FA production [35, 36]. Upregulated genes in high IMF pigs were mostly linked to fat metabolism [37]. Our DEGs exhibited a significant enrichment in pathways linked to the production of fat, for instance AMPK, cAMP, and PPAR signaling pathways. The AMPK signaling pathway affects sterol synthesis, FA and lipolysis, and may influence muscle fiber type transition [38–40]. PPARγ, a key regulator of lipid metabolism and adipocyte differentiation, plays a crucial role in adipogenesis and fat storage [41]. In Laiwu pigs with high IMF content, significant upregulation of PPARγ further supports this finding. PLIN1, an essential protein for intracellular lipid storage, has been identified as a critical player in the regulation of triglyceride hydrolysis and lipid metabolism [42, 43]. Our results indicate that the upregulation of PPARγ, ADIPOQ, PLIN1, SCD, and LEP in Laiwu pigs suggests their involvement in IMF deposition through the regulation of adipogenesis and lipid metabolism. The significant upregulation of these fat deposition-related genes may contribute to the high IMF content in Laiwu pigs.

Lipid composition is associated with the deposition of IMF [44, 45]. Our lipidomics analysis revealed several lipids that may contribute to IMF content, including coenzyme (CO), DG, TG, FA, PG, PE, PC, PS, PI, CL, and ceramides (Cer). PC and PE, the most abundant phospholipids in animal tissues [46], showed a negative correlation with IMF content and slaughter weight in pig muscle [45]. In our study, the levels of PC and PE were low in Laiwu pigs, corresponding to their high IMF content. Furthermore, increased PI levels were observed in Laiwu pigs, which are known to promote lipid droplet formation [47]. These results suggest that elevated PI content in Laiwu pigs may be associated with enhanced IMF deposition. Additionally, Laiwu pigs exhibited high levels of CL (36:3/36:4), potentially linked to a greater proportion of oxidized muscle fibers [48]. Additionally, short- and medium-chain TGs were significantly elevated in Laiwu pigs, while long-chain TGs were more prominent in Yorkshire pigs. Previous studies have identified differential hepatic cell metabolism between fatty and lean pigs [49]. Studies on Duroc × Landrace crossbred

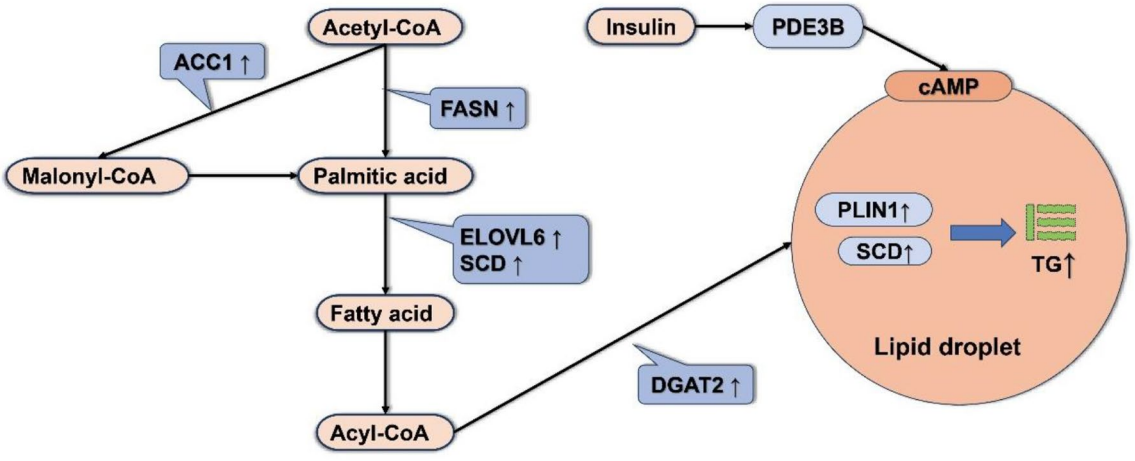

Fig. 7 Correlation and pathway analysis of significantly differential markers with IMF trait. Lipid metabolism processes assigned with DEGs and lipids enriched in KEGG pathways

lean pigs have demonstrated that the liver is the primary organ responsible for the synthesis of long-chain polyunsaturated fatty acids, resulting in increased levels of these fatty acids and their intermediates in pigs [50]. Our findings in Yorkshire pigs further corroborate this observation. Notably, TG16:1–17:1–18:1 and TG16:1–17:1–18:2 as well as TG17:1–18:1–18:2 showed increased levels in the longissimus thoracis muscle of Laiwu pigs, which may contribute to the high lipid deposition in this breed.

Fat deposition is a complex process, and to gain deeper insights into its regulation, we performed an integrated analysis of transcriptomics and lipidomics to identify potential biomarkers closely associated with IMF content. Previous integrated analyses have identified the regulation of meat color through the nicotinic acid and nicotinamide metabolic pathways [51]. It has also been established that DEGs play a more significant role than differentially expressed metabolites in determining IMF deposition [37]. The single lipidomics or transcriptomics analysis might produce accidental error, especially in the case of limited samples. This prompted us to analyze integrated transcriptomics and lipidomics data to better identify functional genes and their regulatory pathways, which are critical for understanding the regulation of intramuscular fat deposition and related metabolic processes. Following the integrated analysis, we observed that DEGs appear to function as upstream regulators influencing IMF deposition, while differential metabolites reflect adaptive responses to varying IMF levels (Fig. 7). Notably, the use of Laiwu and Yorkshire pigs in our study provides a unique comparison, yet further investigation is needed to explore the underlying mechanisms responsible for these breed-specific differences and the potential inconsistencies in regulatory pathways.

Conclusion

The high IMF content in Laiwu pigs was attributed to the coordinated action of gene-lipid interactions, where palmitic acid generated by ACC1 and FASN was elongated and desaturated by ELOVL6 and SCD to form long-chain fatty acids, which were essential for TG synthesis. This process was further facilitated by DGAT2. The synthesized TG was stored in lipid droplets with the help of PLIN1, providing a molecular basis for improving pork quality.

Supplementary Information

The online version contains supplementary material available at https://doi.org/10.1186/s12864-025-11669-9.

Supplementary Material 1

Acknowledgements

This study was financially supported by STI2030-Major Projects (2023ZD0404702) (J.W.), the National Key Research and Development Program of China 2021YFF1000602 (J.W.), the Program for Shaanxi Science and Technology from Shaanxi Provincial Science and Technology Department 2023-CX-TD-57 (J.W.), and Shaanxi Livestock and Poultry Breeding Common Technology Research and Development Platform 2023GXJS-02-01 (J.W.). We would like to express our sincere gratitude for the work of sample collection provided by the whole team at Key Laboratory of Animal Genetics Breeding and Reproduction. We would like to thank Shandong Province Laiwu Pig Original Seed Co., Ltd. (Shandong, China) for their assistance with the feeding of experimental animals.

Author contributions

WCP, GHC, and JWW designed the experiments; WCP, GHC, and JYX performed the experiments and analyzed the data; WCP, JYX, CXZ, and XZ interpreted the results; WCP and JWW wrote the manuscript. During the review process, RRP and YZN made significant contributions to the research of the paper. RRP played a key role in the literature review and manuscript writing, while YZN focused on the validation of the experimental results, the correction of the images, and the revision of the figure notes, which provided important support for the completeness and accuracy of the study. Funding acquisition, JWW. All authors reviewed the manuscript, participated in the discussion, and gave their approval to the final draft of article.

Funding

STI2030-Major Projects (2023ZD0404702) (J.W.). National Key Research and Development Program of China 2021YFF1000602 (J.W.). Program for Shaanxi Science and Technology from Shaanxi Provincial Science and Technology Department 2023-CX-TD-57 (J.W.). Shaanxi Livestock and Poultry Breeding Common Technology Research and Development Platform 2023GXJS-02-01 (J.W.).

Data availability

Availability of data and materialsThe raw sequence data for transcriptomics have been submitted to the NCBI Gene Expression Omnibus (GEO) datasets with accession number GSE268121. The lipidomics data are stored in the EMBL-EBI MetaboLights database (MTBLS10230).

Declarations

Ethics and consent to participate

This study received approval from the Animal Ethics Committee of College of Animal Science & Technology, Northwest A&F University (XN2023-1005). The animals used in our study were purchased by the researchers from Shandong Province Laiwu Pig Original Seed Co., Ltd. (Shandong, China). In accordance with ethical research standards, informed consent was obtained from the owner(s) of the animals prior to their use in the study. The animal owners were fully informed about the nature of the study, the procedures involved, and the potential risks to the animals. We ensured that the welfare of the animals was prioritized throughout the study, in strict adherence to all ethical guidelines.

Consent for publication

Not Applicable.

Competing interests

The authors declare no competing interests.

Received: 23 October 2024 / Accepted: 2 May 2025
Published online: 21 May 2025

References

1. Wood JD, Enser M, Fisher AV, Nute GR, Sheard PR, Richardson RI, Hughes SI, Whittington FM. Fat deposition, fatty acid composition and meat quality: A review. Meat Sci. 2008;78(4):343–58.
2. Wood RJ. Vitamin D and adipogenesis: new molecular insights. Nutr Rev. 2008;66(1):40–6.
3. Munoz M, Garcia-Casco JM, Caraballo C, Fernandez-Barroso MA, Sanchez-Esquiliche F, Gomez F, Rodriguez MDC, Silio L. Identification of candidate genes and regulatory factors underlying intramuscular fat content through longissimus dorsi transcriptome analyses in heavy Iberian pigs. Front Genet. 2018;9:608.

4. Won S, Jung J, Park E, Kim H. Identification of genes related to intramuscular fat content of pigs using genome-wide association study. Asian-Australas J Anim Sci. 2018;31(2):157–62.
5. Katsumata M. Promotion of intramuscular fat accumulation in Porcine muscle by nutritional regulation. Anim Sci J. 2011;82(1):17–25.
6. Bravo-Lamas L, Barron LJR, Farmer L, Aldai N. Fatty acid composition of intramuscular fat and odour-active compounds of lamb commercialized in Northern Spain. Meat Sci. 2018;139:231–8.
7. Guo J, Shan T, Wu T, Zhu LN, Ren Y, An S, Wang Y. Comparisons of different muscle metabolic enzymes and muscle fiber types in Jinhua and landrace pigs. J Anim Sci. 2011;89(1):185–91.
8. Chen W, Fang GF, Wang SD, Wang H, Zeng YQ. Longissimus lumborum muscle transcriptome analysis of Laiwu and Yorkshire pigs differing in intramuscular fat content. Genes Genom. 2017;39(7):759–66.
9. Huang Y, Zhou L, Zhang J, Liu X, Zhang Y, Cai L, Zhang W, Cui L, Yang J, Ji J, et al. A large-scale comparison of meat quality and intramuscular fatty acid composition among three Chinese Indigenous pig breeds. Meat Sci. 2020;168:108182.
10. Zappaterra M, Gioiosa S, Chillemi G, Zambonelli P, Davoli R. Muscle transcriptome analysis identifies genes involved in ciliogenesis and the molecular cascade associated with intramuscular fat content in large white heavy pigs. PLoS ONE. 2020;15(5):e0233372.
11. Zhao X, Hu H, Lin H, Wang C, Wang Y, Wang J. Muscle transcriptome analysis reveals potential candidate genes and pathways affecting intramuscular fat content in pigs. Front Genet. 2020;11:877.
12. Zhang P, Li Q, Wu Y, Zhang Y, Zhang B, Zhang H. Identification of candidate genes that specifically regulate subcutaneous and intramuscular fat deposition using transcriptomic and proteomic profiles in Dingyuan pigs. Sci Rep. 2022;12(1):2844.
13. Wang L, Xie Y, Chen W, Zhang Y, Zeng Y. Identification and functional prediction of long noncoding RNAs related to intramuscular fat content in Laiwu pigs. Anim Biosci. 2022;35(1):115–25.
14. Hou X, Zhang R, Yang M, Niu N, Wu J, Shu Z, Zhang P, Shi L, Zhao F, Wang L, et al. Metabolomics and lipidomics profiles related to intramuscular fat content and flavor precursors between Laiwu and Yorkshire pigs. Food Chem. 2023;404Pt A. 134699.
15. Cesar AS, Regitano LC, Koltes JE, Fritz-Waters ER, Lanna DP, Gasparin G, Mourao GB, Oliveira PS, Reecy JM, Coutinho LL. Putative regulatory factors associated with intramuscular fat content. PLoS ONE. 2015;10(6):e0128350.
16. Mo C, Du Y, O'Connell TM. Applications of lipidomics to Age-Related musculoskeletal disorders. Curr Osteoporos Rep. 2021;19(2):151–7.
17. Ma S, Xia M, Gao X. Biomarker discovery in atherosclerotic diseases using quantitative nuclear magnetic resonance metabolomics. Front Cardiovasc Med. 2021;8:681444.
18. Xia B, Cai GH, Yang H, Wang SP, Mitchell GA, Wu JW. Adipose tissue deficiency of hormone-sensitive lipase causes fatty liver in mice. PLoS Genet. 2017;13(12):e1007110.
19. Wen B, Mei Z, Zeng C, Liu S. MetaX: a flexible and comprehensive software for processing metabolomics data. BMC Bioinformatics. 2017;18(1):183.
20. Kuhl C, Tautenhahn R, Bottcher C, Larson TR, Neumann S. CAMERA: an integrated strategy for compound spectra extraction and annotation of liquid chromatography/mass spectrometry data sets. Anal Chem. 2012;84(1):283–9.
21. Smith CA, Want EJ, O'Maille G, Abagyan R, Siuzdak G. XCMS: processing mass spectrometry data for metabolite profiling using nonlinear peak alignment, matching, and identification. Anal Chem. 2006;78(3):779–87.
22. Dieterle F, Ross A, Schlotterbeck G, Senn H. Probabilistic quotient normalization as robust method to account for Dilution of complex biological mixtures. Application in 1H NMR metabonomics. Anal Chem. 2006;78(13):4281–90.
23. Chen M, Zhang C, Li H, Zheng S, Li Y, Yuan M, Chen Y, Wu J, Sun Q. PLA2G4A and ACHE modulate lipid profiles via glycerophospholipid metabolism in platinum-resistant gastric cancer. J Transl Med. 2024;22(1):249.
24. Sander LC. Soxhlet extractions. J Res Natl Inst Stand Technol. 2017;122:1.
25. Shi XC, Xia B, Zhang JF, Zhang RX, Zhang DY, Liu H, Xie BC, Wang YL, Wu JW. Optineurin promotes myogenesis during muscle regeneration in mice by autophagic degradation of GSK3beta. Plos Biol. 2022;20(4):e3001619.
26. Duan Y, Zheng C, Zheng J, Ma L, Ma X, Zhong Y, Zhao X, Li F, Guo Q, Yin Y. Profiles of muscular amino acids, fatty acids, and metabolites in shazi-ling pigs of different ages and relation to meat quality. Sci China Life Sci. 2023;66(6):1323–39.
27. Hu H, Wang J, Zhu R, Guo J, Wu Y. Effect of myosin heavy chain composition of muscles on meat quality in Laiwu pigs and duroc. Sci China C Life Sci. 2008;51(2):127–32.
28. Zheng A, Rahkila P, Vuori J, Rasi S, Takala T, Vaananen HK. Quantification of carbonic anhydrase III and myoglobin in different fiber types of human Psoas muscle. Histochemistry. 1992;97(1):77–81.
29. Hwang YH, Kim GD, Jeong JY, Hur SJ, Joo ST. The relationship between muscle fiber characteristics and meat quality traits of highly marbled Hanwoo (Korean native cattle) steers. Meat Sci. 2010;86(2):456–61.
30. Picard B, Gagaoua M, Micol D, Cassar-Malek I, Hocquette JF, Terlouw CE. Inverse relationships between biomarkers and beef tenderness according to contractile and metabolic properties of the muscle. J Agric Food Chem. 2014;62(40):9808–18.
31. Wood JD, Enser M, Fisher AV, Nute GR, Richardson RI, Sheard PR. Manipulating meat quality and composition. Proc Nutr Soc. 1999;58(2):363–70.
32. Karlsson AH, Klont RE, Fernandez X. Skeletal muscle fibers as factors for pork quality. Livest Prod Sci. 1999;60(2–3):255–69.
33. Renand G, Picard B, Touraille C, Berge P, Lepetit J. Relationships between muscle characteristics and meat quality traits of young Charolais bulls. Meat Sci. 2001;59(1):49–60.
34. Jeong DW, Choi YM, Lee SH, Choe JH, Hong KC, Park HC, Kim BC. Correlations of trained panel sensory values of cooked pork with fatty acid composition, muscle fiber type, and pork quality characteristics in Berkshire pigs. Meat Sci. 2010;86(3):607–15.
35. Munoz G, Alves E, Fernandez A, Ovilo C, Barragan C, Estelle J, Quintanilla R, Folch JM, Silio L, Rodriguez MC, et al. QTL detection on Porcine chromosome 12 for fatty-acid composition and association analyses of the fatty acid synthase, gastric inhibitory polypeptide and acetyl-coenzyme A carboxylase alpha genes. Anim Genet. 2007;38(6):639–46.
36. Pena RN, Ros-Freixedes R, Tor M, Estany J. Genetic marker discovery in complex traits: A field example on fat content and composition in pigs. Int J Mol Sci 2016, 17(12).
37. Hou X, Zhang R, Yang M, Niu N, Zong W, Yang L, Li H, Hou R, Wang X, Wang L, et al. Characteristics of transcriptome and metabolome concerning intramuscular fat content in Beijing black pigs. J Agric Food Chem. 2023;71(42):15874–83.
38. Guo Z, Chen X, Huang Z, Chen D, Li M, Yu B, He J, Luo Y, Yan H, Zheng P. Dihydromyricetin improves meat quality and promotes skeletal muscle fiber type transformations via AMPK signaling in growing-finishing pigs. Food Funct. 2022;13(6):3649–59.
39. Chen X, Guo Y, Jia G, Liu G, Zhao H, Huang Z. Arginine promotes skeletal muscle fiber type transformation from fast-twitch to slow-twitch via Sirt1/AMPK pathway. J Nutr Biochem. 2018;61:155–62.
40. Li HW, Chen XL, Chen DW, Yu B, He J, Zheng P, Luo YH, Yan H, Chen H, Huang ZQ. Ellagic acid alters muscle Fiber-Type composition and promotes mitochondrial biogenesis through the AMPK signaling pathway in healthy pigs. J Agr Food Chem. 2022;70(31):9779–89.
41. Christofides A, Konstantinidou E, Jani C, Boussiotis VA. The role of peroxisome proliferator-activated receptors (PPAR) in immune responses. Metabolism. 2021;114:154338.
42. Gol S, Ros-Freixedes R, Zambonelli P, Tor M, Pena RN, Braglia S, Zappaterra M, Estany J, Davoli R. Relationship between perilipin genes polymorphisms and growth, carcass and meat quality traits in pigs. J Anim Breed Genet. 2016;133(1):24–30.
43. Tansey JT, Sztalryd C, Gruia-Gray J, Roush DL, Zee JV, Gavrilova O, Reitman ML, Deng CX, Li C, Kimmel AR, et al. Perilipin ablation results in a lean mouse with aberrant adipocyte lipolysis, enhanced leptin production, and resistance to diet-induced obesity. Proc Natl Acad Sci U S A. 2001;98(11):6494–9.
44. Li J, Zhang J, Yang Y, Zhu J, He W, Zhao Q, Tang C, Qin Y, Zhang J. Comparative characterization of lipids and volatile compounds of Beijing Heiliu and Laiwu Chinese black pork as markers. Food Res Int. 2021;146:110433.
45. Li J, Yang YY, Zhan TF, Zhao QY, Zhang JM, Ao X, He J, Zhou JC, Tang CH. Effect of slaughter weight on carcass characteristics, meat quality, and lipidomics profiling in longissimus thoracis of finishing pigs. Lwt-Food Sci Technol 2021, 140.
46. Dannenberger D, Nuernberg G, Scollan N, Ender K, Nuernberg K. Diet alters the fatty acid composition of individual phospholipid classes in beef muscle. J Agric Food Chem. 2007;55(2):452–60.
47. Chorlay A, Monticelli L, Verissimo Ferreira J, Ben M, Ajjaji K, Wang D, Johnson S, Beck E, Omrane R, Beller M. Membrane asymmetry imposes directionality on lipid droplet emergence from the ER. Dev Cell. 2019;50(1):25–e4227.
48. Schlame M, Rua D, Greenberg ML. The biosynthesis and functional role of Cardiolipin. Prog Lipid Res. 2000;39(3):257–88.

49. Gonzalez-Valero L, Rodriguez-Lopez JM, Lachica M, Fernandez-Figares I. Metabolic differences in hepatocytes of obese and lean pigs. Animal. 2014;8(11):1873–80.
50. Duran-Montge P, Theil PK, Lauridsen C, Esteve-Garcia E. Fat metabolism is regulated by altered gene expression of lipogenic enzymes and regulatory factors in liver and adipose tissue but not in semimembranosus muscle of pigs during the fattening period. Animal. 2009;3(11):1580–90.
51. Zhan H, Xiong Y, Wang Z, Dong W, Zhou Q, Xie S, Li X, Zhao S, Ma Y. Integrative analysis of transcriptomic and metabolomic profiles reveal the complex molecular regulatory network of meat quality in Enshi black pigs. Meat Sci. 2022;183:108642.

Publisher's note